Turbulence Suppression in Discharges with Off-Axis ECRH on T-10 Tokamak Device.

D. A. Shelukhin, V. A. Vershkov, K. A. Razumova

Nuclear Fusion Institute RRC "Kurchatov Institute", Moscow, Russia

E-mail: shelukhin@nfi.kiae.ru

Abstract. Transient steep electron temperature gradient has been observed in T-10 tokamak plasmas at ρ = 0.25 immediately after off-axis Electron Cyclotron Resonance Heating (ECRH) switch off. The turbulence characteristics were investigated in these discharges by means of correlation reflectometry. It was found that density fluctuations amplitude was 2 times lower than Ohmic level in narrow region near ρ = 0.25 after ECRH switch off. Poloidal coherency of fluctuations is also decreased in this region. Suppression of quasi-coherent oscillations has been observed in considered discharges during strong temperature gradient existence. Turbulence poloidal rotations measurements showed no any velocity shear after ECRH switch-off. Analysis of the linear growth rates of instabilities shows that Ion Temperature Gradient (ITG) mode is unstable at $\rho \sim 0.25$ during all discharge. Possible explanation of the observed phenomena is the rational surface density decrease near q = 1 due to q profile transient flattering after off-axis ECRH switch off.

1. Introduction

Investigation of discharges with off-axis ECRH is very interesting from physical point of view. First of all off-axis ECRH broadens electron temperature and current density profiles which leads to sawteeth oscillations suppression that is very convenient for plasma physics investigations in central part of plasma column. Off-axis ECRH gives the opportunity to form flat electron temperature profiles in the central part of plasma column also. This effect should lead to turbulence suppression due to Critical Gradient Models (CGM). Besides that, previous experiments on T-10 tokamak device showed electron transport barrier formation in transient phase of discharge after ECRH switch off.

This work presents the recent results of turbulence investigations in discharges with off-axis ECRH on T-10. The paper organized in following way: the experimental setup, used diagnostics and main plasma parameters are described in the second part. The third part deals with turbulence investigations in observed discharges. The estimations of transport coefficients are given in the fourth part. The results of experiments are discussed in fourth part of paper. The summary of work is given in the conclusion.

2. Experimental set up.

The discussed experiments with off axis ECRH were carried out on T-10 tokamak device [1]. T-10 has a circular cross section with major radius R = 1.5 m and minor radius a = 0.3 m. The plasma current was about I_p = 180 kA and toroidal magnetic field was B_T = 2.33 T in main experiments. The line averaged electron density slightly varied from 1.5 to $2 \cdot 10^{19}$ m^{-3}. Additional experiments with different plasma current and toroidal magnetic field were made to justify the observed effects. The target plasma was heated with two gyrotrons with total power about 0.53 MWt at frequency 140 GHz. It corresponds to strong off-axis (at ρ = 0.4) ECRH heating at second harmonic of EC frequency.

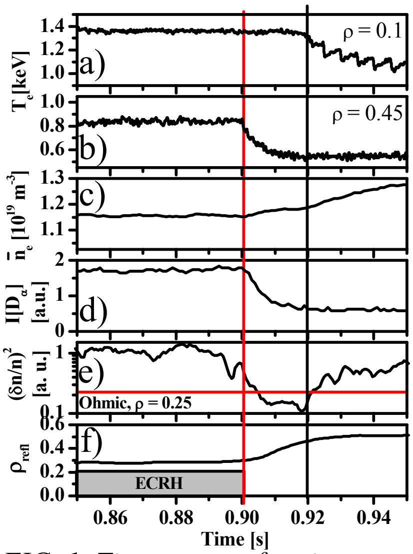

FIG. 1. Time traces of various plasma parameters in discharge with off-axis EXRH

The electron temperature was measured using multi channel second harmonic ECE radiometer. The absolute value of electron temperature was calculated by calibration of radiometer signals in Ohmic phase of discharge obtained from the slope of the soft x-ray spectra with Pulse Height Analysis. Electron density was measured by 8-channel radio-interferometer as well as by 8-channel HCN-laser interferometer. Data from both diagnostics were used for reliable plasma density profile reconstruction.

The plasma turbulence was measured with O-mode correlation heterodyne reflectometer [2]. It has the opportunity to register the reflected wave parameters at three different poloidal positions so it is possible to determine relative amplitude of electron density fluctuations, poloidal coherency of fluctuations and poloidal velocity of these fluctuations.

The discharge scenario was as follows – at 0.5 s of discharge after current and electron density ramp up the off-axis ECRH began. It continues about 350 ms and after ECRH switch off there was a stage of pure Ohmic heating with duration about 100 ms. The typical time traces of different plasma characteristic in considered discharges are shown on figure 1. It is clearly seen that the electron temperature in the heated region ($\rho \sim 0.45$) is decreased immediately after off-axis ECRH switch off (red vertical line) (Fig. 1 b). In the same time the temperature in plasma center remains unchanged during 10-20 ms after ECRH switch off (Fig. 1 a). After that, the central temperature decreases due to sawteeth activity appearance.

Such plasma behavior leads to formation of strong electron temperature gradient just inside the heated region. The characteristic electron temperature profiles for discussed discharges are shown in figure 2 a (points correspond to measured positions, lines - to the temperature approximation). One should see that temperature profile during ECRH is wider then in the Ohmic phase of discharge (respectively blue and red symbols and lines). The characteristic profile parameter R/L_{Te} is changed at $\rho \sim 0.2$ from 4 during ECRH to 6 for Ohmic case. However, in the transient phase of discharge the strong electron temperature gradient with $R/L_{Te} \sim 15$ is seen (green symbols and lines). This value is higher that critical value of electron temperature gradient predicted by CGM so one should expect strong turbulence and transport level in this plasma region [3]; thus this approach contradicts to long temperature retaining in the plasma center. It should be also noted that the region of the strong electron temperature gradient coincides with observed position of sawteeth phase change in Ohmic phase of discharge. This position is usually considered as radial position of q = 1 magnetic surface.

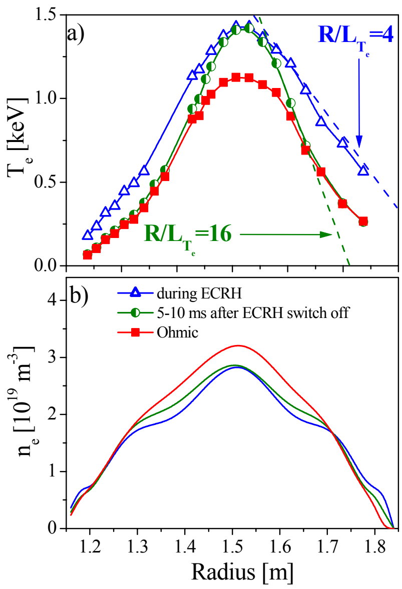

FIG. 2. Electron temperature and density profile in discharges with off-axis ECRH

The behavior of line averaged electron density in these experiments was typical for ECRH heated discharges on T-10 (Figure 1. c). It begins to rise immediately after ECRH switch off. The careful reconstruction of electron density profiles shows that profile was peaked inside the heated region and this was the only possibility to carry out density fluctuation measurements in this plasma region (figure 2 b, blue line). This peak remains for some time after ECRH switch off (fig. 2 b, green line) and then profile relaxes to Ohmic (red line). Special consideration shows that this peak is not artificial; it is seen on raw interferometer data also. The neutrals influx controlled by monitor D_α spectral line intensity from both rail limiter (fig. 1 d). It shows strong increase during ECRH and rapid decrease after ECRH switch off.

3. Turbulence measurements.

Plasma turbulence was measured by means of small-scale electron density measurements by O-mode correlation heterodyne reflectometer. As the reflectometer has a fixed frequency in each discharge the measurements was carried out in a series of reproducible discharges at different reflectometer frequencies to obtain radial profiles of turbulence characteristics. Small changes of electron density were used also to make more accurate turbulence characteristics profiles measurements. The reflection layer position was changed during the discharge due to density profile variation so we used the reconstructed electron density profile to determine the reflection position. Usual variation of reflection level position during discharge is shown in figure 1 f. The density fluctuations amplitude was calculated from quadrature (vector) registration of reflected signal electric field. The correction for non-locality of reflectometer measurements was made using 1D geometric approach [4].

The typical time trace of electron density perturbations level in frequency band [50 ÷ 400] kHz is shown in figure 1 e. The turbulence level during ECRH is much higher that the Ohmic values and greatly decreased after ECRH switch off for a time period about 10 ms. Moreover the density fluctuations during this period is about 2 times lower than in Ohmic phase of discharge at the equal radial position which is shown by red line.

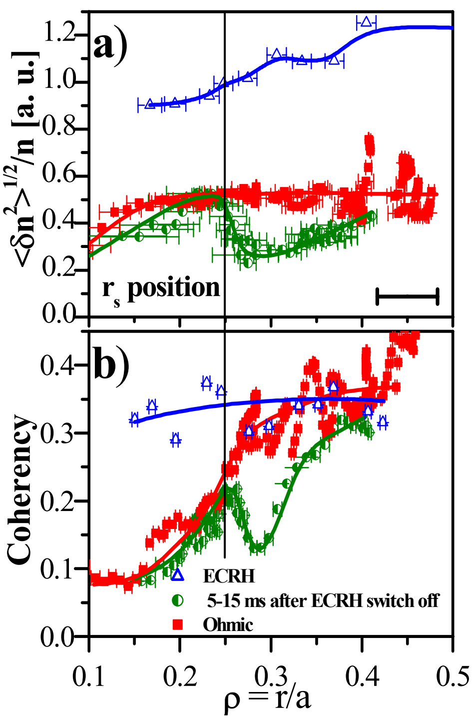

FIG. 3. Profiles of density fluctuations amplitude and poloidal coherency

The radial profile of density fluctuations amplitude was measured as described above and averaged over three registered channels. The results are presented in figure 3 a. One can see that the level of density fluctuations in Ohmic discharge is practically constant in gradient region (red points and line). The fluctuations level is strongly (2 ÷ 4 times) increased during off-axis ECRH in the whole plasma core. This means that even in the weak electron temperature gradient region inside the heated zone the turbulence lever exceeds the Ohmic level. This fact contradicts to Critical Gradient Model of turbulence. During 5 - 15 ms after ECRH switch off density fluctuations level decreased to the Ohmic value at all observed radii except the narrow region near $\rho \sim 0.3$, where it drops two

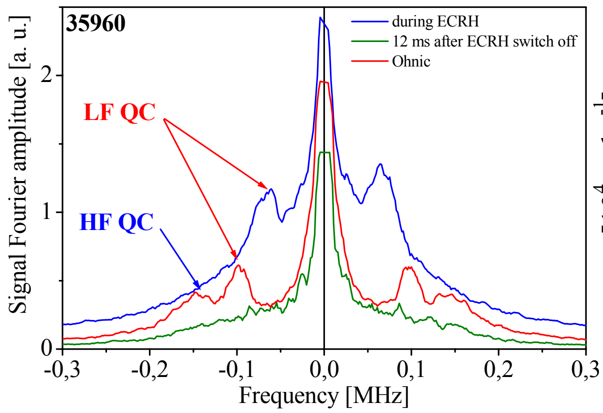

FIG. 4. Fourier spectra of reflectometer signal for different time in discharge

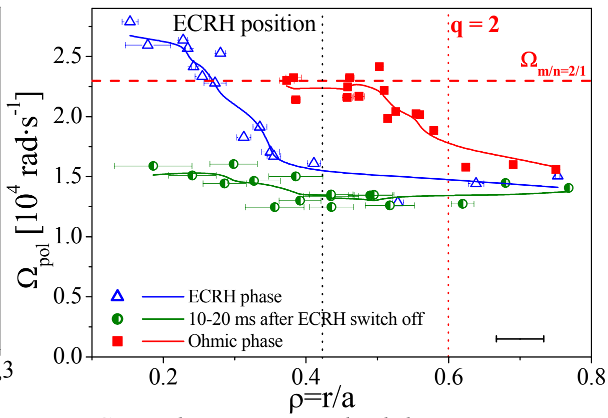

FIG. 5. Fluctuations poloidal rotation velocity in ECRH, transitional and Ohmic phase of discharge.

times lower the Ohmic level. The absolute position is in sufficiently good agreement with strong electron gradient position because of about 2 cm uncertainty in reflection layer radial position due to the errors in density profile reconstruction.

The correlation measurements is also shown that the poloidal coherency level in the region of density fluctuation suppression decreased in time interval 5 ÷ 20 ms after ECRH switch off in 4 times with respect to the level during ECRH (figure 3 b, green and blue points and lines respectively). This points out that the poloidal correlation length decrease after ECRH switch off. The correlations level during Ohmic phase of discharge (red points and line) is slightly higher than during ECRH.

The careful look at the turbulence spectra could give the additional information about mechanism of observed phenomena. The figure 4 shows the typical turbulence amplitude Fourier spectra near $\rho \sim 0.3$ for three moments of time: during ECRH (blue line), 5-15 ms after ECRH (green one) and in Ohmic phase of discharge (red one). One can see that during ECRH the density perturbations spectrum has a strong level of Broad Band (BB) fluctuations. It has also peak of Low Frequency (LF) Quasi Coherent (QC) oscillations at the frequency about 100 kHz. It should be noted that such spectra was previously found to be characteristic for the regimes with strong particle flow [5]. After ECRH switch off the turbulence level decreases in high frequency band and no evidence of LF QC oscillations appears in the spectra. These facts point to the strong turbulence stabilization mechanism in the temperature gradient region. The BB level relax to Ohmic value after strong electron temperature gradient degradation. Both LF and High Frequency (HF) QC oscillations is seen in signal spectrum in this phase of discharge.

Density fluctuation suppression is often observed in transport barrier on other devices [6]. The universal mechanism of this suppression is the turbulence stabilization by velocity shear [7]. The turbulence velocity in discussed experiments on T-10 was measured by means of poloidal delay determination from cross correlation function. As the poloidal separation of reflection points is known it was able to determine the angular velocity. The results are presented in figure 5. The velocity in Ohmic phase is constant in the plasma core (red points and line) – region inside q = 2 magnetic surface (position of q = 2 is shown by dotted red line). The interesting fact is that the turbulence velocity in this region is close to the rotation velocity of m/n = 2/1 MHD island (horizontal dashed red line). The turbulence rotation outside the q = 2 surface is about 2 times slower. The velocity profile during ECRH is similar to the Ohmic one but the strong velocity gradient position moves to the plasma center (blue points and line). It could be explained in the following way: the electron transport in the ECR heated plasma increases and absolute value of plasma potential drops. It leads to the radial electric field decrease and slowing of E × B rotation. After ECRH switch off turbulence velocity decreases along the all observed radii and forms uniform profile (green points and line). This means that the velocity shear stabilization could not explain observed phenomena. The reflectometry measurements in similar discharge show the same turbulence behavior in other discharges with strong off-axis ECRH.

4. Transport studies in discharges with off-axis ECRH

The transport coefficients in discharges with off-axis ECRH on T-10 were already analyzed with various methods. The analysis based on the cold pulse propagation showed that electron heat conductivity χ_e inside $\rho \sim 0.3$ decrease lower than 0.3 m^2/s after ECRH switch off [8]. More complicated model was based upon the temperature time trace analysis [9]. This method gives the values of χ_e about 0.25 m^2/s inside the heated region and narrow zone ($\Delta\rho \sim 0.05$) with minimum heat conductivity about 0.15 m^2/s.

Unfortunately, both methods analyzed the effective electron thermal conductivity and not take into account the heat flux due to particle transport. As it was stressed above the turbulence spectra form during ECRH could be explained by strong charge particle fluxes. Full information could be drawn out of heat balance equation. The total heat flux in this case is represented in the following form:

$$\Gamma_e = -n_e \chi_e \frac{\partial T_e}{\partial r} + \frac{3}{2}\Gamma_n T_e = -n_e\left[\chi_e + \chi_e^{diff}\right]\frac{\partial T_e}{\partial r} = -n_e \chi_e^{eff}\frac{\partial T_e}{\partial r},$$

where χ_e^{diff} has a sense of effective heat conductivity due to the particle flux and determined such as:

$$\chi_e^{diff} = \frac{3}{2}\frac{\Gamma_n T_e}{n_e}\left(\frac{\partial T_e}{\partial r}\right)^{-1}.$$

The experimental data was analyzed using ASTRA 1.5D code [10]. The experimental profiles of electron temperature and density, loop voltage and total ECRH power were used in simulation. It was used also the ECRH power deposition profile determined by Andreev *et al* [9]. The time dependence of neutral influx was determined from D_α line intensity. Absolute value of neutral influx was chosen in the way to get the ratio of heat conductivity to particle diffusion coefficient $\chi_e/D_e \sim 2$ for the Ohmic phase of discharge. The obtained value of particle influx not contradicts to previously measured values. The Spitzer current conductivity was chosen to calculate the Ohmic heat source and current diffusion. The ion temperature calculated in the following assumptions: the heat transmission from electrons to ion is neoclassical; the radial profile of ion heat conductivity is neoclassical multiplied by a factor of 2 – 3 to agree the simulated value of ion temperature and neutral flux with experimental ones. It was found that

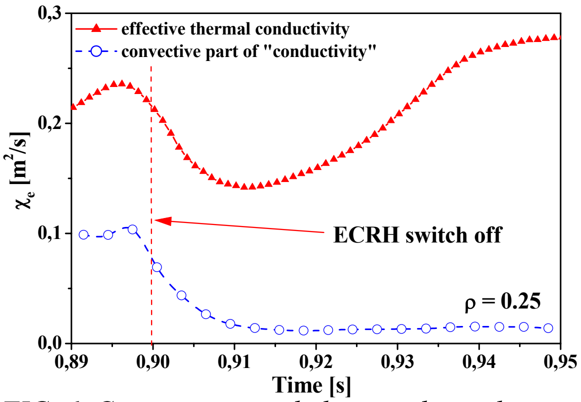

FIG. 6. Comparison total electron thermal conductivity with convective term

the analysis of heat balance equation gives values of heat conductivity coefficient close to the value obtained by other methods. The interesting data could be obtained by analysis of heat flux structure. Figure 6 shows the comparison of total effective heat conductivity χ_e^{eff} (red line) with the effective heat conductivity due to the particle flux χ_e^{diff} (blue line) at the radius where the strong electron temperature gradient observed. It is clearly seen that a considerable part of a heat flux during ECRH is transferred by particle. It happens due to the strong neutrals flux from both wall and rail limiter during ECRH and deep penetration of these neutrals in these discharges. After ECRH switch off the neutral flux is dramatically drops down and the effective heat conductivity decrease. Then χ_e^{eff} relaxes to the Ohmic value.

5. Discussion.

The experimental facts shows that in considered discharges after off-axis ECRH switch off the following phenomena are observed: strong gradient of electron temperature, suppression of small-scale density fluctuations and low level of electron transport coefficients. Thus, we could consider these as the electron Internal Transport Barrier (ITB) evidences. The main question is the physical mechanism of its formation. As it was discussed above the stabilization by velocity shear is impossible because of a flat turbulence velocity profile.

Another possible mechanism of instabilities stabilization could be the decrease of instabilities increments. The estimation of heat conductivity was made from real electron temperature and density profiles and calculated ion temperature and q value from linear theory. Previous investigations show that main contributions for fluctuations in the plasma core are come from Ion Temperature Gradient (ITG) instability and Dissipative Trapped Electron Mode (DTEM) [11]. The heat conductivity for ITG was calculated as proposed in [12] and the DTEM contribution estimation was based on [13].

The results are presented on the figure 7 a. The calculation was made for three time moments – during off-axis ECRH (blue line), 5-15 ms after ECRH switch off (green line) and for the Ohmic discharge (red line). Solid lines correspond to the ITG and dashed lines to the DTEM contributions. One can see that ITG transport is prevailed in the plasma center during all discharge. The estimated heat conductivity remains the same after ECRH switch off near barrier. It could be easily understood as the ion temperature and density profile inside this region not change dramatically which leads to the constant transport. Interesting fact is that the DTEM instability region should move to the plasma center. It correlates with appearance of HF QC oscillations peak in plasma center in Ohmic phase (figure 4, red line).

Thus, the linear instabilities theory approach cannot explain full set of experimental data. The experiments with off-axis ECRH showed that the formation of this barrier could be very sensitive to the q profile [1]. So, the approach based on the magnetic configuration was used to estimate the transport coefficients [14]. The plasma transport in this model is the result of the interaction of narrow radially localized modes with high poloidal m and toroidal n numbers. Each mode with m, n numbers located at r_m^n gives the following impact in plasma transport:

$$\chi_{sp}^{n,m}(r - r_m^n) = \chi_0 \cdot \exp\left[-0.5\left[\left(r - r_m^n\right)/\rho_i\right]^2\right],$$

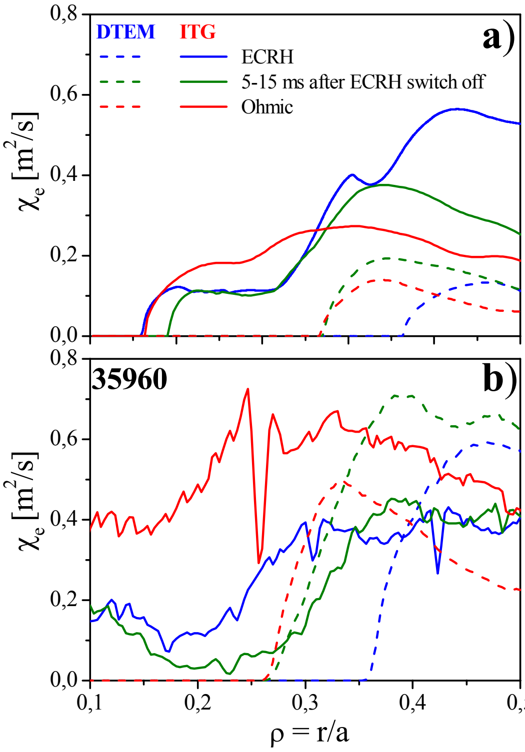

FIG. 7. Comparison of theoretical estimations of heat diffusivity from linear theory (a) and taking into account the magnetic configuration (b)

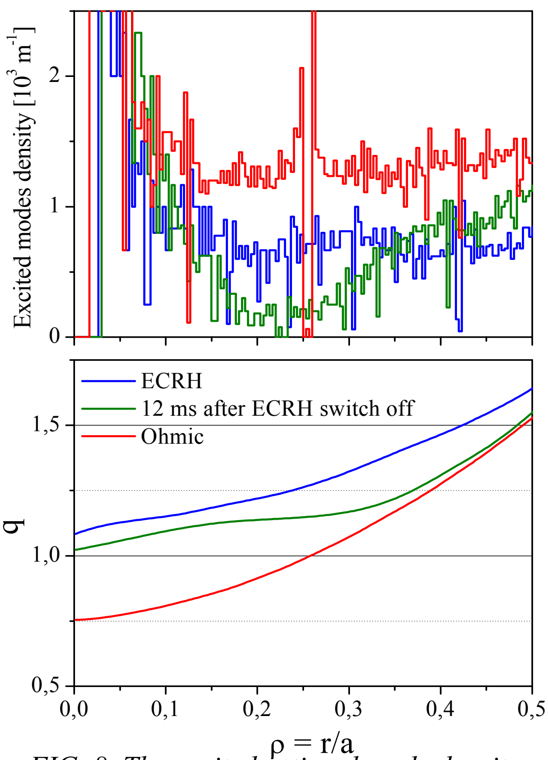

FIG. 8. The excited rational mode density (a) and q value profile in discharge with off-axis ECRH due to [1] (b).

where χ_0 is the heat conductivity of instability in linear theory, ρ_i – ion Larmour radius. The authors of [14] propose to calculate the resulting transport by summation of all m, n modes. It leads to strong transport increase to the plasma edge that is much higher than experimentally observed values. We propose the following modification of this method. The transport is caused by coupling of modes with different poloidal but the same toroidal number. The resulting transport is calculated by averaging for all possible toroidal numbers:

$$\chi^n(r) = \sum_m \chi_{sp}^{n,m}(r) \qquad\qquad \chi(r) = \sum_n \chi^n(r) / n_{\max}(r) .$$

The maximum poloidal and toroidal numbers was determined by the corresponding instabilities conditions. The $k_\perp \cdot \rho_i$ value was chosen to be equal 0.3 for ITG and 1 to DTEM. Thus the maximum poloidal and toroidal number was taken in a form:

$$m_{\max}(r) = k_\perp r \qquad\qquad n_{\max}(r) = m_{\max}(r) / q(r) .$$

Plasma transport in proposed approach is proportional to the “excited mode density” that has sense of the averaged number of rational magnetic surfaces with the same toroidal n number in fixed radial interval. Calculated excited mode density is presented in figure 8 a. The q profiles for calculations was taken from [1] and presented in figure 8 b. Blue lines correspond to the off-axis ECRH phase of discharge, red one – to the Ohmic one and green one to the moment about 12 ms after ECRH switch off on both plots. It is clearly seen that density of magnetic surfaces is practically uniform along all interesting radius in both ECRH and Ohmic phase of discharge. In contrast, it has a minimum near $\rho \sim 0.2$ after ECRH switch off. The position of this minimum corresponds to the region of low gradient on q profile. It occurs because number of rational surfaces with high m, n numbers decreased near low m/n q value. In conditions of low gradient of q in this region the magnetic surfaces are separated on the distance that exceeds their radial size so the coupling become impossible and it leads to transport reduction.

The calculated transport coefficient values are presented in figure 7 b. The legend is the same as on the fig. 7 a. One can see that the heat conductivity is strongly decreased after ECRH switch off. Moreover, this approach could explain the disappearance of quasi-coherent oscillations after barrier formation. The formation of radially elongated structures that is seen as quasi-coherent oscillations is the toroidal coupling of modes on excited rational magnetic surfaces. If the toroidal coupling is broken by any mechanism (velocity shear or strong radial mode separation) quasi coherent oscillations vanish.

6. Summary

Strong electron temperature gradient was found on T-10 tokamak device after off-axis ECRH switch off. The transport coefficient was low (about 0.15 – 0.3 m^2/s) and the density fluctuation suppression was observed in this region. It allows to consider temporary ITB formation in discussed discharges. It was shown that most popular mechanism of instability stabilization by velocity shear is not take place. It was proposed the new approach to explain the barrier formation based on the decreasing of high m/n number magnetic surfaces near low m/n magnetic surface in conditions of low magnetic shear. The proposed mechanism is rather raw and more accurate consideration and simulation required.

The authors would like to thank S. V. Soldatov and A. O. Urasbaev for help in reflectometer operating, M. V. Osipenko and A. D. Beklemishev for fruitful discussions and T-10 operating team. This work was supported by grants: Scientific School 1608.2003.2, NWO-RFBR 047.009.009, RFBR 04-02-17562, RFBR 04-02-17567 and INTAS 2001-2056.

[1] K.A. Razumova *et al*, Nuclear Fusion **44** (2004), 1067
[2] V.A. Vershkov *et al*, 1999, RSI, V. 70, N. 3, 2903.
[3] F.Ryter et al, 19th IAEA Fusion Energy Conference, Lyon, France, 2002, IAEA-CN-94/EX/P3-04
[4] E.Mazzucato, R.Nazikian, Phys. Rev. Lett. **71**, 1840 (1993).
[5] V.A. Vershkov *et al*, 30 EPS Conference on Contr. Fusion and Plasma Phys., St. Petersburg, Russia (2003) ECA Vol. 27A, P3-115
[6] G.D. Conway, *et al*., Phys Rev Letters **84** 1463 (2000)
[7] C.M. Greenfield *et al*, Phys Plasmas **4** 1596 (1997)
[8] S.V. Neudatchin *et al*, 2003 EPS Conf. Plasma Phys. Cont. Fus.
[9] V.F. Andreev *et al*, 2004 Plasma Phys. Control. Fusion 46. 319
[10] G.V. Pereverzev and P.N. Yushmanov 2002 ASTRA: an Automated System for Transport Analysis in a Tokamak. Max-Planck Institute Report, IPP 5/98.
[11] V.A. Vershkov *et al*, 31 EPS Conference on Contr. Fusion and Plasma Phys., London, UK (2004) ECA, P1-172
[12] M.Z. Tokar *et al*, 2000, Phys. Rev. Lett., 84, 895
[13] J. Weiland, H. Nordman, Nuclear Fusion, 31, (1991), 390
[14] A.D. Beklemishev, W. Horton, Phys Fluids B 4 (1), 1992